MICROBIAL ECOLOGY

Microb Ecol (2002) 43:416–423
DOI: 10.1007/s00248-001-1063-z

Elongation Correlates with Nutrient Deprivation in *Pseudomonas aeruginosa*–Unsaturated Biofilms

R.E. Steinberger,[1] A.R. Allen,[2] H.G. Hansma,[2] P.A. Holden[1]

[1] Donald Bren School of Environmental Science and Management, University of California, Santa Barbara, CA 93106, USA
[2] Department of Physics, University of California, Santa Barbara, CA 93106, USA

Received: 1 October 2001; Accepted: 21 December 2001; Online publication: 8 April 2002

ABSTRACT

Bacteria in nature frequently grow as biofilms, yet little is known regarding how biofilm bacteria morphologically adapt to low nutrient availability, which is common in unsaturated environments such as the terrestrial subsurface or on plant leaves. For unsaturated biofilms, in which the substratum may provide all nutrients, what are the relationships between nutrition and cell size and shape—the simplest metrics of cellular morphology? To address this question, we cultured *Pseudomonas aeruginosa,* a ubiquitous gram-negative bacterium that is environmentally and medically important, on membranes overlaying solid media, and then measured cellular dimensions using atomic force microscopy (AFM). Nutrition was controlled chemically by media composition and physically by stacking membranes to increase the path length for nutrient diffusion. Under conditions of carbon–nitrogen imbalance, low carbon bioavailability, or increased nutrient diffusional path length, cells elongated while maintaining constant width. A mathematical relationship suggests that, by elongating, biofilm bacteria strategically enlarge their nutrient collection surface without substantially changing the ratio of surface area to volume (SA/V). We conclude that *P. aeruginosa* growing as unsaturated biofilm with a planar nutrient source morphologically adapt to starvation by elongating. This adaptation, if generalizable, differs from a better-understood starvation response (i.e., cell size decreases; thus SA/V increases) for planktonic bacteria in well-mixed environments.

Introduction

Bacteria have evolved to take maximum advantage of physical and chemical changes in their environment. Natural environments such as soils, sediments, and marine and freshwaters on average have very limited carbon and energy sources because of the continual depletion of these resources by microbes [15]. In liquid culture, changing nutrient availability has been demonstrated to stimulate changes in cell shape. In their classic experiment, Schaechter et al. demonstrated that exponential-phase *Salmonella typhimurium* grown in rich media were wider and heavier than cells grown in minimal media [29].

Correspondence to: R.E. Steinberger; Phone: (805) 893-5652; Fax: (805) 893-7612; E-mail: rsteinberger@bren.ucsb.edu

Mathematically, the proportion of cell length to width was relatively constant, which led Zaritsky to define it as the shape factor, *R* [37]. Similar results have been shown in *Escherichia coli* [17, 36]. At the other end of the nutritional scale, cells subjected to starvation during exponential phase became much smaller and rods changed shape to become cocci [7, 14, 23]. However, unlike laboratory liquid culture, most real-world growth environments are not well-mixed. Indeed, when bacteria grow as biofilms, dense consortia of surface-associated bacteria embedded in organic polymers [6], mass transport of nutrients is often rate-limiting [5]. Because surface-associated growth is generally recognized as the most common mode of bacterial growth in nature and disease [10] and because biofilms often form under nutrient-limited conditions [5], understanding how bacterial cells change size and shape in response to nutrient limitation in unmixed systems is fundamental to microbial ecology.

Several experimenters growing biofilms have observed an unexplained pattern of filamentous growth, even in monocultures of rod-shaped bacteria. A mixture of *Pseudomonas putida* and *P. fluorescens* degrading a mixture of low molecular weight aromatic chemicals grew as long stringy cells when attached to the solid support of a bioreactor but as short rods in liquid culture [30]. Similarly, a *Pseudomonas* isolate elongated when grown as a biofilm under oligotrophic conditions, but not when grown in oligotrophic liquids or when grown on a surface under nutrient-rich conditions [25]. In normally rod-shaped *S. typhimurium,* mutations in the elongation genes *rodA* and *mre* are lethal to biofilm cells but not planktonic cells [9]. This suggests that in the biofilm mode of growth, the maintenance of a rod shape has some unique importance. Filamentous cells are frequently found in biofilms causing high frictional resistance in fluid systems [25]. This makes the understanding of filamentous cells in biofilms under nutrient-limited conditions important for industrial purposes [25]. Furthermore, like biofilms in flowing systems, bacteria growing in unsaturated environments (e.g., in soil [11, 28], on root surfaces [11], on leaf and food surfaces, as colonies) are surface-associated and embedded in a polymer matrix, and thus can be named unsaturated biofilms. Anomalous growth behavior such as unexpected filamentous growth can make microscopic classification of bacteria in both saturated and unsaturated biofilms difficult [3]. However, the general relationship between cell morphology and nutritional conditions in poorly mixed environments is unknown, as is an explanation for the observation that starved *Pseudomonas* species elongate in biofilms but not in liquid culture [25, 30].

In this work, we studied the relationship between nutrient deprivation and cell morphology for *P. aeruginosa,* an environmentally and medically important bacterium. By cultivating cells on membranes overlying chemically controlled solid media or by varying the number of membranes to control the path length for nutrient diffusion, we were able to simulate a range of nutritional conditions common to unsaturated environments. Analysis of images acquired by atomic force microscopy (AFM) provided cellular dimensions from which cell surface area (SA) and volume were calculated. Statistical comparisons were made for the various growth conditions and a mathematical model is presented which both explains our findings and provides an explanation for prior reports of filamentous cells in biofilms.

Methods

The method used to cultivate our unsaturated biofilms differs markedly from the more traditional biofilm cultivation techniques that rely on flow cells to mimic the fluid shear occurring in saturated environments. Our method is intended to simulate the environment (no fluid shear, three-phase system) with nutrient gradients and zones of depletion as are expected to develop in a poorly mixed system [26] such as soil.

Strain, Media, and Cultivation

P. aeruginosa strain PG201 (Urs Ochsner, University of Colorado) was maintained at −80°C in 70% Luria–Bertani (LB) broth/30% glycerol. Solid media were prepared from an aqueous mineral stock containing 0.5 g NH_4Cl, 1.725 g $Na_2HPO_4 \cdot 7H_2O$, and 1.38 g KH_2PO_4 per liter [16] and solidified with 1.5% Bacto-Agar (Difco, Fisher Scientific, Pittsburgh, PA). Trace minerals were supplied by adding 40 mL per liter of filter-sterilized (0.2 μm) Hutner's mineral solution [31] after autoclaving and prior to dispensing into standard petri dishes. The carbon to nitrogen ratio (C/N) was controlled by the amount of carbon source. When glucose was the carbon source, it was added to the aqueous mineral media from a 0.34 g/mL solution to achieve C/N ratios of 1, 11, and 24. Hexadecane, an alternative carbon source, was dispensed as an 18% filter-sterilized (0.2 μm) solution in hexane onto the solid media surface. The hexane was allowed to volatilize completely.

Nuclepore® polyester membranes (13 mm diameter, 0.1 μm pore, 6 μm thick, Whatman, Clifton, NJ) were individually sterilized with 70% ethanol for 2 min, air-dried, then transferred with

sterile forceps to the solid media surface. For treatments in which nutrient diffusional path length was controlled, 1, 2, or 3 membranes were stacked and the underlying solid medium was comprised of solidified mineral media supplemented with glucose (C/N = 11).

Membranes were inoculated by transferring a small amount of frozen stock directly to the membrane surface using a sterile pick. The inoculated membranes overlying solid media were incubated at 30°C for approx. 16 h before harvesting. The biofilms grew radially and concentrically away from the point of inoculation. All treatments were independently triplicated.

Sample Harvesting and Microscopy

Membranes with biofilm were removed intact from the agar surface using sterile forceps. The membranes, with biofilm oriented upward, were transferred to double-sided sticky carbon tabs (Ted Pella, Inc., Redding, CA) and then onto steel disks. Samples were air-dried for approximately 30 min in a sterile flow hood. Drying has been shown to improve AFM imaging without changing cell morphology [1]. AFM images of biofilms after 30 min and after several days were similar.

The biofilms were imaged in tapping mode, using a Dimension 3000 AFM (Digital Instruments, Santa Barbara, CA), under ambient conditions. Silicon cantilevers with resonant frequencies of ca. 300 kHz were used. Scan rates were ca. 2.5 Hz.

Cell Measurement and Data Analysis

Using Nanoscope software (Digital Instruments), cells were measured across the center from the lowest point on each side (between the cell and its neighbor, Fig. 1B). Fields of cells were selected for measurement along the edges of the biofilm to minimize capturing the morphological variability that might occur along a radial axis from the center to the edge of the biofilm as a consequence of nutrient depletion in the densest regions [27]. Each cell was considered an individual data point. Between 15 and 45 cells were measured on each membrane. Cells were mathematically modeled as rectangular boxes; thus the cellular SA and volume (V) are:

$$\mathrm{SA} = (2l \cdot w) + (2l \cdot d) + (2w \cdot d) \tag{1}$$

$$V = l \cdot w \cdot d \tag{2}$$

where l is length, w is width, and d is depth. Using the assumption that the depth is proportional to width by a proportionality factor n,

$$d = n \cdot w \tag{3}$$

Equations (1) through (3) are combined to calculate the ratio of surface area to volume (SA/V):

$$\frac{\mathrm{SA}}{V} = \frac{2 + 2n}{n} \cdot \frac{1}{w} + 2 \cdot \frac{1}{l} \tag{4}$$

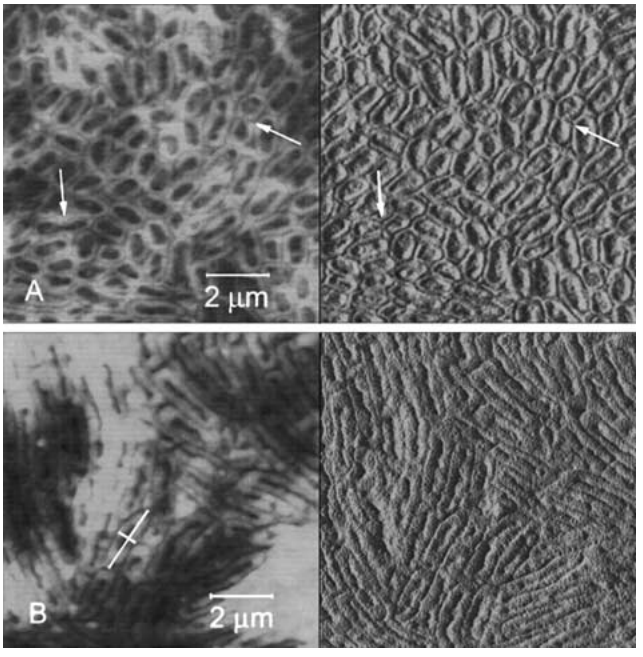

Fig. 1. Unsaturated *Pseudomonas aeruginosa* biofilms imaged by AFM. Shown are height (left) and amplitude (right) images representing a 10-μm square of biofilm. Relative to the cells of the control treatment (A), cells in the low bioavailability (hexadecane-grown) biofilm (B) are noticeably elongated. Cells with central constrictions (white arrows) were thought to be dividing and were not measured. The white cross bar in (B) indicates how the length and width of each cell was measured.

Similar results can be obtained by assuming cylindrical geometry, but the bacteria appeared relatively flat making rectangular boxes an acceptably simple conceptual model. Where equations included a depth term, we assumed that depth is equal to width (i.e., $n = 1$). As long as $n \leq 1$, our calculations that depend on this assumption are valid. Pairwise comparisons for the treatments were conducted using single-factor ANOVA performed using Excel 2000®. The measurement error associated with width and length was propagated through all calculations using accepted methods [33].

Results

Nutritional Effects on Cell Morphology

Unsaturated biofilms were grown under conditions of carbon limitation, nitrogen limitation, and low carbon bioavailability. Our control medium used glucose as a carbon source and had a C/N of 11, very close to the ratio dictated by a generalized formula ($C_5H_7NO_2$) for bacteria [13] assuming one-half of the glucose is mineralized. The

carbon-limited (C/N = 1) and nitrogen-limited (C/N = 24) media used differing amounts of glucose to control C/N. Hexadecane was used as a carbon source to limit carbon availability by low aqueous solubility.

As has been seen previously, AFM provides detailed, high-resolution images of unsaturated biofilms relatively nondestructively [1]. In our samples, cells were easily identified as bright, smooth, rectangular outlines with slightly rounded corners (Fig. 1). In all treatments, the dark color in the centers of the cells indicates that cell centers are lower than the edges. This is either a natural feature or due to a loss of cell turgor pressure upon drying. Particularly for our control treatment (glucose as a carbon source, C/N = 11), symmetric central constrictions were sometimes evident (Fig. 1A, white arrows), indicating cellular division.

We measured the lengths and widths of the cells for several images per sample, always defining the length as the larger distance. Because the cells were so closely packed and were likely thicker than the AFM tip length, absolute depth could not be measured. However, since actively growing *Pseudomonas* are rod-shaped bacteria, the cell depth is nearly the same as the width. The carbon-limited (C/N = 1) and nitrogen-limited (C/N = 24) cells were longer than control cells, which grew at a balanced C/N. Otherwise, the biofilms appeared similar. When biofilms were cultivated using hexadecane (Fig. 1B) instead of glucose (Fig. 1A), cells were also significantly elongated. As compared to the control, the cell boundaries were not as crisply defined and appeared thicker when hexadecane was the carbon source. Also when hexadecane was the carbon source, no significant difference in cell length was observed for different C/N ratios (data not presented), reflecting the control of low aqueous solubility on C bioavailability.

For each treatment, the coefficient of variation (CV) for the lengths was approx. 20–25% and the CV for the widths was 10–15%, showing an expected level of variation in individual cell size [8]. However, there was no correlation between the length and widths of individual cells, though such correlations have previously been reported [34]. The average cell widths for all the treatments were between 0.64 μm and 0.66 μm (Fig. 2) and did not vary significantly ($p > 0.1$). The average cellular lengths resulting from different nutritional treatments (Fig. 2) were all significantly different ($p < 0.001$) with the control cells being the shortest (1.40 ± 0.03 μm) followed by the carbon-limited (1.62 ± 0.04 μm), nitrogen-limited (1.87 ± 0.05 μm), and hexadecane-grown (low bioavailability) cells (2.52 ± 0.09 μm).

Effects of Nutrient Diffusional Path Length

Biofilms were cultivated overlying several membranes to elucidate the effect of increasing the nutrient diffusional path length on cell size. Diffusional path length significantly influenced cell length but not cell width (Fig. 3). Biofilm cells cultivated on 1 membrane (approx. 6 μm thick) had the shortest average length (1.396 ± 0.034 μm). Cells in biofilms cultivated on 2 membranes were longer (2.076 ± 0.047 μm) but not as long as cells in biofilms overlying 3 membranes, which had an average length of 2.650 ± 0.074 μm. The length of the cells was a linear function ($r^2 = 0.998$) of the number of underlying membranes or total path length. Biofilm cellular response to the increased diffusional distance was extremely similar to the response to poor nutrition, suggesting a common response to a common treatment factor in all these experiments.

Modeled Cell SA, Volume, and SA/V

Small cells, like bacteria, have large SA/V. With a larger SA/V, the cell can exchange materials with the environment more efficiently, precluding the need for complicated internal transport systems [4, 24]. Using Equations (1)–

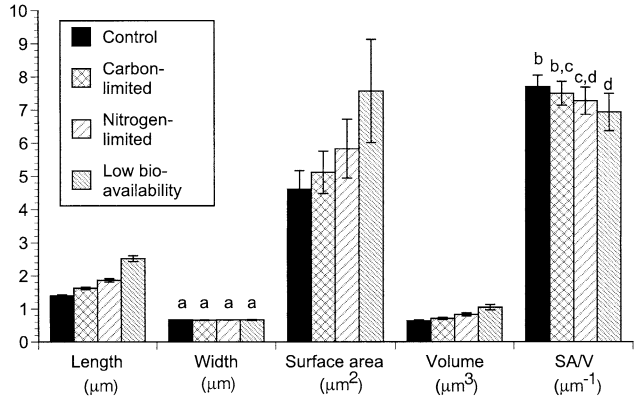

Fig. 2. Average dimensions for biofilm cells grown under different nutritional conditions. Error bars represent the standard error of the mean. Bars labeled with c's or d's are not significantly different ($p > 0.05$) and bars labeled with a's or b's are not significantly different ($p > 0.10$). Unlabeled bars are statistically unique; i.e., they vary significantly from all other bars within the dimension category ($p < 0.02$). Treatments were: control (C/N = 11), carbon-limited (C/N = 1), nitrogen-limited (C/N = 24), and low bioavailability (hexadecane).

(4), we calculated the SA, volume, and SA/*V* for all treatments. In the nutrition experiments, the SA increased dramatically when the low bioavailability treatment (7.57 ± 1.56 μm^2) was compared to the control (4.60 ± 0.56 μm^2). The SA values of the carbon-limited (5.11 ± 0.64 μm^2) and the nitrogen-limited treatments (5.83 ± 0.88 μm^2) were intermediate. The cellular SA increased with the number of membranes, from 4.60 ± 0.56 μm^2 for biofilms cultivated on 1 membrane, to 6.34 ± 0.85 μm^2 and 7.59 ± 1.33 μm^2 for biofilms cultivated on 2 and 3 membranes, respectively. The average cellular volume was smallest for the control biofilms (0.627 ± 0.029 μm^3) and largest for hexadecane-grown biofilms (1.043 ± 0.080 μm^3). The average cellular volume for carbon-limited (0.703 ± 0.033 μm^3) and nitrogen-limited biofilms (0.828 ± 0.047 μm^3) was intermediate. Biofilms cultivated on 3 membranes had a larger average cellular volume (1.098 ± 0.072 μm^3) than biofilms cultivated on 1 (0.627 ± 0.029 μm^3) or 2 membranes (0.907 ± 0.045 μm^3). Across all treatments, the average SA and average cellular volume varied by 40–80% of the mean values (Figs. 2, 3).

In contrast, the average SA/V varied only slightly with treatment. The average cellular SA/V (7.69 ± 0.35 μm^{-1}) for control biofilms was slightly larger than that of carbon-limited (7.49 ± 0.36 μm^{-1}), nitrogen-limited (7.27 ± 0.41 μm^{-1}), and hexadecane-grown biofilms (6.93 ± 0.56 μm^{-1}). However, cellular SA/V varied by only 0.75 μm^{-1} across treatments, which is approximately 10% of the calculated mean. Smaller variations in the average cellular SA/V were observed between biofilms cultivated on 1 (7.69 ± 0.35 μm^{-1}), 2 (7.15 ± 0.37 μm^{-1}), and 3 membranes (7.18 ± 0.51 μm^{-1}). Using pairwise comparison, the cellular SA/V were statistically the same ($p > 0.05$) for four treatments. The average cellular SA and volume varied significantly ($p < 0.02$) across all treatments. Despite the significant differences in both the average cellular SA and volume, SA/V is relatively constant.

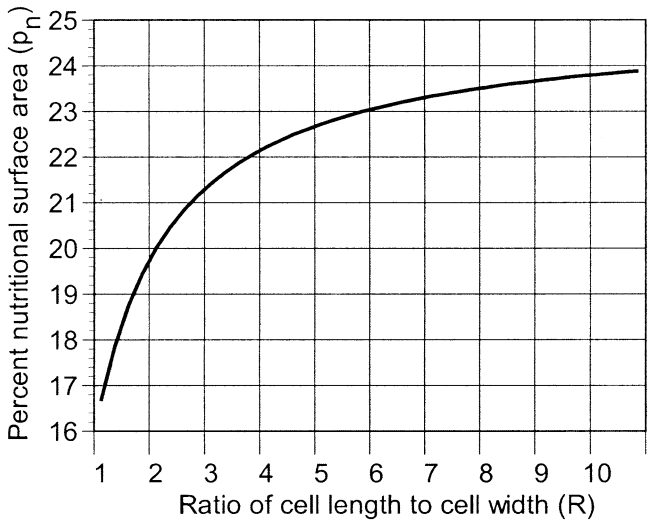

Fig. 4. Percentage of the total surface area (p_n) that is nutrient-providing versus the ratio (*R*) of cell length to cell width for cells growing on a nutrient-providing surface.

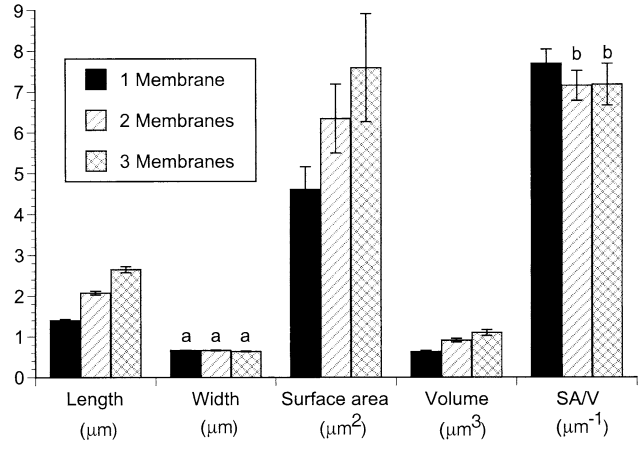

Fig. 3. Average dimensions for biofilm cells cultivated on 1, 2, and 3 membranes overlying glucose-amended solid medium, C/N = 11. Error bars represent the standard error of the mean. Bars labeled with a's or b's are not significantly different ($p > 0.1$). Unlabeled bars are statistically unique; i.e., they vary significantly from all other bars ($p < 0.01$).

Discussion

We examined bacterial cellular morphology in unsaturated biofilms as a function of nutrition. We demonstrated that biofilm cells grow longer but not wider when one nutrient (C or N) is scarce because of an imbalanced nutrient ratio or poorly bioavailable carbon source. Similarly, cell lengths increased with increasing distances separating the bacteria from their nutrient source, which decreases nutrient flux according to Fick's law. Approximate cellular SA and volumes were calculated from the length and width measurements by modeling the cells as rectangular boxes. The changes in cell lengths altered the SA and volume more significantly than the SA/V.

A close examination of the mathematics illustrates that SA/V values are relatively constant when they are calculated from a changing cell length and relatively constant cell width. In Equation (4), two fractions are added to-

gether to determine SA/V, the first dependent solely on width and the second dependent solely on length. We assume that n, the ratio of depth to width, will always be less than or equal to 1 since gravity exerts force only on cellular depth and not width. Thus the coefficient of the width-dependent term in Equation (4) will have a minimum value of 4 and will always exceed the coefficient of the length-dependent term, 2. Furthermore, since the length is always greater than the width, the inverse of the length will always be less than the inverse of the width. The larger coefficient of the width-dependent term and the larger inverse of the width in Equation (4) guarantee that the width-dependent fraction will dominate SA/V. Given that we saw no significant differences in width, it is not surprising that SA/V did not vary with treatment.

The changes in length without changes in width lead to the obvious question: what advantage do longer biofilm cells have on suboptimal media? One possible advantage is that longer cells have more area oriented toward the nutrient-supplying media below. Except oxygen, all required nutrients originate in the underlying solid medium. Thus most of the cell's nutrients must diffuse to the biofilm cells through the bottom cellular faces. Because of the closely packed arrangement of cells in our biofilm, the cells behave as part of a macroscopic whole, with nutrient flux being proportional to the bottom surface area [21, 22]. Nutrient gathering per cell increases as the cellular SA increases. We define the nutrient-providing surface area of the cell, SA_n, as the surface area oriented towards the nutrient source. The SA_n is always some percentage, p_n, of the total SA of the cell:

$$SA_n = \frac{p_n}{100} \cdot SA \tag{5}$$

In liquid, because the cell is bathed in its nutrient-providing medium, all of the cellular SA is nutrient-gathering, which means $p_n = 100\%$ and $SA_n/V = SA/V$. However, in biofilm cells, only one face (the bottom) of each cell is oriented toward the nutrient source and, therefore, nutrient-gathering. Thus:

$$p_n = \frac{SA_n}{SA} \cdot 100 = \frac{l \cdot w}{(2 + 2n)(l \cdot w) + (2n \cdot w^2)} \cdot 100 \tag{6}$$

We substitute Zaritsky's shape factor, R, defined in equation (7), to obtain a simplified expression for p_n, shown in Equation (8).

$$R = \frac{l}{w} \tag{7}$$

$$p_n = \frac{R}{(2 + 2n)R + 2n} \cdot 100 \tag{8}$$

This relation, graphed in Fig. 4, clearly shows that longer cells (i.e. those with higher R) have a higher proportion of their SA oriented toward the solid media. This means that total cellular SA is used more efficiently for nutrient gathering. If nutrient-limited sessile cells shrank down to cocci ($R = 1$) as many nutrient-limited cells in liquid culture do, their calculated p_n would decrease to 16.7%. In theory, biofilm cells can convert an additional 8% of their surface area to be nutrient-providing by infinitely increasing their length. However, in a classic case of diminishing returns, the benefit of increasing p_n decreases as the length increases relative to the width (Fig. 4). Increasing from a coccus ($R = 1$) to a short rod ($R = 2$) provides the same 3% increase in p_n as an increase from a short rod ($R = 2$) to a very long rod ($R = 7$).

These results question how applicable a classic paradigm in general microbiology is to biofilms: that starvation leads to decreases in cell size and thereby increases SA/V. This paradigm, tested for nutritional conditions ranging from starved ultra-microbacteria [15] to cells in rich broth [29], states that because smaller cells have higher SA/V ratios, they can sequester nutrients more efficiently. However, most studies relating nutritional conditions to cell size have been carried out in liquid culture, where nutrients are provided evenly over the entire cell surface (i.e., $SA_n = SA$) and SA/V is identical to SA_n/V.

The elongation of biofilm cells when grown with a strongly directional nutrient source has been observed in both this paper and other work [25, 30]. Gradients of nutrient availability are generally expected to occur near interfaces. In papers by Kjelleberg et al. [20] and James et al. [18], though, starvation of bacteria at interfaces reduced the average cell size. These interfaces are more sparsely colonized and the majority of bacteria are not in physical contact with other bacteria. However, even though the average cell size at the interface was less than in the bulk phase, the largest cells were found at the interface [20] suggesting that elongation could have occurred in some interfacial cells. The different responses observed may be due to the difference in diffusion in biofilm, a macroscopic system where nutrient flux is

proportional to surface area [21, 22], and diffusion around isolated cells, which are microscopic systems where nutrient flux is proportional to cell length [2]. Thus, whether elongation occurs may be partially density-dependent. Further testing is also needed to determine whether other species of bacteria elongate as a result of nutrient stress or if this response is unique to *Pseudomonas* species.

Although elongation was clearly observed in response to nutrient stress, other stresses may also stimulate elongation. In liquid culture, cells enlarge in response to elevated temperatures [8], swell with osmotic upshock [12, 19], and often elongate with antibiotics [35]. The direct activity of the stressor may be responsible for changes in cell size, as has been demonstrated for osmotic stress [12, 19] and antibiotics [35], but in unsaturated systems, such as soil, many stresses indirectly influence nutrient availability. For example, soil desiccation can result in low nutrient availability since water is the solvent in which nutrients are transported to the cells [32]. Similarly, increasing or decreasing the temperature changes the rate of diffusion and thereby increases or decreases the rate of nutrient resupply. The pervasiveness of nutrient stress in natural environments, whether alone or in combination with other stresses, may explain the high degree of general stress resistance starved cells exhibit [14]. By focusing on nutrient stress in the absence of other stressors, we were able to isolate the biofilm cellular response to what is likely to be a common underlying stress in most soil systems. Further research is needed to determine whether elongation is a more general stress response that may occur from other individual stressors or many stressors acting in concert.

There have been previous reports that, under poor nutritional conditions, bacteria growing in biofilms assume a fibrous mode of growth [25, 30]. Poor nutrition can result from a variety of causes, including nutrient imbalance, poor bioavailability, and increased physical separation from the nutrient source, all of which have been demonstrated in this paper. In the fibrous mode of growth, *P. aeruginosa* significantly and noticeably increase their average length while the cell widths remain constant. In theory, this increases the percentage of cellular surface area oriented toward a planar nutrient source. This is analogous to the increase in SA/*V* observed for starved cells in liquid culture, but clearly growth-habit-dependent. The increase in SA_n seems to be a compensatory mechanism for the decreased flux of nutrients to the cell, possibly explaining the phenomenon of fibrous growth in biofilms.

Acknowledgements

Funding for this project was provided by the U.S. Environmental Protection Agency Fellowship No. U915832-01 to R.E. Steinberger, National Science Foundation Award No. 9982743 to H.G. Hansma, and the U.S. Environmental Protection Agency Award No. R827133-01 to P.A. Holden and A.A. Keller. We thank John Sitko and Issayas Afework for their valuable technical assistance in imaging and analyzing the biofilms.

References

1. Auerbach ID, Sorensen C, Hansma HG, Holden PA (2000) Physical morphology and surface properties of unsaturated *Pseudomonas putida* biofilms. J Bacteriol 182:3809–3815
2. Berg HC (1983) Random Walks in Biology. Princeton University Press, Princeton, NJ
3. Bottone EJ, Thomas CA, Lindquist D, Janda JM (1995) Difficulties encountered in identification of a nutritionally deficient streptococcus on the basis of its failure to revert to streptococcal morphology. J Clinical Microbiol 33:1022–1024
4. Brock TD (1966) Principles of Microbial Ecology. Prentice-Hall, Englewood Cliffs, NJ
5. Characklis WG (1990) Process analysis. In: WG Characklis, KC Marshall (eds) Biofilms. John Wiley & Sons, Inc, New York, pp 93–130
6. Characklis WG, Marshall KC (1990) Biofilms: a basis for an interdisciplinary approach. In: WG Characklis, KC Marshall (eds) Biofilms. John Wiley & Sons, Inc, New York, pp 3–15
7. Clegg CD, Van Elsas JD, Anderson JM, Lappin-Scott HM (1996) Survival of parental and genetically modified derivatives of a soil isolated *Pseudomonas fluorescens* under nutrient-limiting conditions. J Appl Bacteriol 81:19–26
8. Cooper S (1991) Bacterial Growth and Division: Biochemistry and Regulation of Prokaryotic and Eukaryotic Division Cycles. Academic Press, San Diego
9. Costa CS, Anton DN (1999) Conditional lethality of cell shape mutations of *Salmonella typhimurium: rodA* and *mre* mutants are lethal on solid but not in liquid medium. Curr Microbiol 38:137–142
10. Costerton JW, Lewandowski Z, Caldwell DE, Korber DR, Lappin-Scott HM (1995) Microbial biofilms. Ann Rev Microbiol 49:711–745
11. Foster RC, Rovira AD, Cock TW (1983) Ultrastructure of the Root–Soil Interface. American Phytopathological Society, St. Paul, MN

12. Galinski EA (1995) Osmoadaptation in bacteria. In: RK Poole (ed) Advances in Microbial Physiology, vol 37. Academic Press, London, pp 273–328
13. Gaudy AFJ, Gaudy ET (1980) Microbiology for Environmental Scientists and Engineers. McGraw-Hill Book Company, New York
14. Givskov M, Eberl L, Moller S, Poulsen LK, Molin S (1994) Responses to nutrient starvation in *Pseudomonas putida* KT2442: Analysis of general cross-protection, cell shape, and macromolecular content. J Bacteriol 176:7–14
15. Gottschal JC (1992) Substrate capturing and growth in various ecosystems. J Appl Bacteriol Symp Suppl 73:39S–48S
16. Guirard BM, Snell EE (1981) Biochemical Factors in Growth. In: P Gerhardt, RGE Murray, RN Costilow, EW Nester, WA Wood, NR Krieg, GB Phillips (eds) Manual of Methods for General Bacteriology. ASM, Washington DC
17. Helmstetter C, Cooper S, Pierucci O, Revelas E (1968) On the bacterial life sequence. Cold Spring Harbor Symp Quant Biol 33:809–822
18. James GA, Korber DR, Caldwell DE, Costerton JW (1995) Digital image analysis of growth and starvation responses of a surface-colonizing *Acinetobacter* sp. J Bacteriol 177:907–915
19. Jennings DH (1990) Osmophiles. In: C Edwards (ed) Microbiology of Extreme Environments. McGraw-Hill Publishing Company, New York, pp 117–146
20. Kjelleberg S, Humphrey BA, Marshall KC (1982) Effect of interfaces on small, starved marine bacteria. Appl Environ Microbiol 43:1166–1172
21. Kooijman SALM, Muller EB, Stouthamer AH (1991) Microbial growth dynamics on the basis of individual budgets. Antonie van Leeuwenhoek 60:159–174
22. Kreft J-U, Booth G, Wimpenny JWT (1998) BacSim, a simulator for individual-based modeling of bacterial colony growth. Microbiology (Reading) 144:3275–3287
23. Lappin-Scott HM, Cusack F, Macleod A, Costerton JW (1988) Starvation and nutrient resuscitation of *Klebsiella pneumoniae* isolated from oil well waters. J Appl Bacteriol 64:541–550
24. Madigan MT, Martinko JM, Parker J (2000) Brock Biology of Microorganisms, 9th ed. Prentice Hall, Upper Saddle River, NJ
25. McCoy WF, Costerton JW (1982) Fouling biofilm development in tubular flow systems. Dev Industrial Microbiol 23:441–448
26. Nedwell DB, Gray TRG (1987) Soils and sediments as matrices for microbial growth. In: M Fletcher, TRG Gray, JG Jones (eds) Ecology of Microbial Communities, vol 41. Cambridge University Press, New York, pp 21–54
27. Pirt SJ (1975) Principles of Microbe and Cell Cultivation. Blackwell Scientific, Oxford, UK
28. Roberson EB, Firestone MK (1992) Relationship between desiccation and exopolysaccharide production in a soil *Pseudomonas* sp. Appl Environ Microbiol 58:1284–1291
29. Schaechter M, Maaloe O, Kjeldgaard NO (1958) Dependency on medium and temperature of cell size and chemical composition during balanced growth of *Salmonella typhimurium*. J Gen Microbiol 19:592–606
30. Shim H, Yang S-T (1999) Biodegradation of benzene, toluene, ethylbenzene, and *o*-xylene by a coculture of *Pseudomonas putida* and *Pseudomonas fluorescens* immobilized in a fibrous-bed bioreactor. J Bacteriol 67:99–112
31. Smibert RM, Krieg NR (1981) General characterization. In: P Gerhardt, RGE Murray, RN Costilow, EW Nester, WA Wood, NR Krieg, GB Phillips (eds) Manual of Methods for General Bacteriology. ASM, Washington DC
32. Soil Science Society of America (1981) Water Potential Relations in Soil Microbiology. Soil Science Society of America, Madison, WI
33. Taylor JR (1997) An Introduction to Error Analysis: The Study of Uncertainties in Physical Measurements, 2nd ed. University Science Books, Sausalito, CA
34. Trueba FJ, Woldringh CL (1980) Changes in cell diameter during the division cycle of *Escherichia coli*. J Bacteriol 142:869–878
35. Umbreit WW (1976) Essentials of Bacterial Physiology. Stroudsburg, PA, Dowden, Hutchinson, & Ross, Inc
36. Van De Merwe WP, Li Z-Z, Bronk BV, Czege J (1997) Polarized light scattering for rapid observation of bacterial size changes. Biophys J 73:500–506
37. Zaritsky A (1975) On dimensional determination of rod-shaped bacteria. J Theor Biol 54:243–248